water

MDPI

Review

Direct and Activated Chlorine Dioxide Oxidation for Micropollutant Abatement: A Review on Kinetics, Reactive Sites, and Degradation Pathway

Xiaohong Ma [1,2], Huan Chen [3,*], Ruihuan Chen [4] and Xiaojun Hu [5,*]

[1] School of Geography and Environment Science, Northwest Normal University, Lanzhou 730070, China; xhma1029@nwnu.edu.cn
[2] Key Laboratory of Resource Environment and Sustainable Development of Oasis, Lanzhou 730070, China
[3] Department of Environmental Engineering and Earth Science, Clemson University, Clemson, SC 29634, USA
[4] College of Life and Environmental Science, Wenzhou University, Wenzhou 325035, China; rhchen@wzu.edu.cn
[5] School of Chemical and Environmental Engineering, Shanghai Institute of Technology, Shanghai 201418, China
* Correspondence: huanc@clemson.edu (H.C.); hu-xj@mail.tsinghua.edu.cn (X.H.)

Abstract: Recently, ClO_2-based oxidation has attracted increasing attention to micropollutant abatement, due to high oxidation potential, low disinfection byproduct (DBPs) formation, and easy technical implementation. However, the kinetics, reactive sites, activation methods, and degradation pathways involved are not fully understood. Therefore, we reviewed current literature on ClO_2-based oxidation in micropollutant abatement. In direct ClO_2 oxidation, the reactions of micropollutants with ClO_2 followed second-order reaction kinetics (k_{app} = 10^{-3}–10^{6} M^{-1} s^{-1} at neutral pH). The k_{app} depends significantly on the molecular structures of the micropollutant and solution pH. The reactive sites of micropollutants start with certain functional groups with the highest electron densities including piperazine, sulfonyl amido, amino, aniline, pyrazolone, phenol groups, urea group, etc. The one-electron transfer was the dominant micropollutant degradation pathway, followed by indirect oxidation by superoxide anion radical ($O_2^{\bullet-}$) or hydroxyl radical ($^{\bullet}OH$). In UV-activated ClO_2 oxidation, the reactions of micropollutants followed the pseudo-first-order reaction kinetics with the rates of 1.3×10^{-4}–12.9 s^{-1} at pH 7.0. Their degradation pathways include direct ClO_2 oxidation, direct UV photolysis, ozonation, $^{\bullet}OH$-involved reaction, and reactive chlorine species (RCS)-involved reaction. Finally, we identified the research gaps and provided recommendations for further research. Therefore, this review gives a critical evaluation of ClO_2-based oxidation in micropollutant abatement, and provides recommendations for further research.

Keywords: Chlorine Dioxide (ClO_2); micropollutant; kinetics; degradation pathway; reactive sites

check for updates

Citation: Ma, X.; Chen, H.; Chen, R.; Hu, X. Direct and Activated Chlorine Dioxide Oxidation for Micropollutant Abatement: A Review on Kinetics, Reactive Sites, and Degradation Pathway. *Water* **2022**, *14*, 2028. https://doi.org/10.3390/w14132028

Academic Editor: Yijing Shi

Received: 19 May 2022
Accepted: 22 June 2022
Published: 24 June 2022

1. Introduction

The micropollutants also known as contaminants of emerging concerns (CECs) are comprised of various anthropogenic and natural compounds, such as pharmaceuticals and personal care products (PPCPs), endocrine disruptors, and pesticides [1,2]. Their presence in natural and engineered systems, even at trace concentrations (ng L^{-1} to μg L^{-1}), has attracted significant attention because of their toxic, persistent, bioaccumulative properties [3]. Due to increased industrialization and urbanization, many micropollutants are widely used, and eventually end up in different types of wastewaters. Unfortunately, traditional wastewater treatment plants (WWTPs) are not explicitly designed for micropollutant abatement, resulting in WWTPs being one of the significant sources of micropollutants in surface water [4]. Until now, various techniques have been proposed for micropollutant abatement in WWTPs, including activated carbon/biochar adsorption [5], advanced oxidation processes (AOPs) [6,7], and membrane filtration [8]. AOPs have attracted growing

attention among these techniques because of their simple operation, high removal efficiency, and rapid oxidation.

AOPs enable an approach combining two individual processes of disinfection and decontamination with improved cost-effectiveness [9,10]. Chlorine Dioxide (ClO_2) is a green disinfectant/oxidant and was listed as an A1-level, safe, and efficient disinfectant by the World Health Organization (WHO) [11]. It has been prevalently used as a drinking water disinfectant alternative to chlorine (Cl_2) due to its effectiveness in pathogen inactivation and limited formation of halogenated disinfection byproducts (DBPs), such as trihalomethanes (THMs) and haloacetic acids (HAAs) [12]. In addition, the products of ClO_2 disinfection/oxidation consist 50–70% of chlorite (ClO_2^-) and 30–50% of chlorate (ClO_3^-) and chloride (Cl^-) [13,14]. Controlling the levels of these ClO_2 residuals is critical for successfully implementing ClO_2 disinfection/oxidation.

Recently, ClO_2-based oxidation for micropollutant abatement has attracted increased attention due to its advantages of strong oxidation, low DBPs formation, and easy technical implementation. ClO_2 can effectively oxidize micropollutants with electron-rich functional groups such as aniline, phenolic, aromatic, and tertiary amine groups [15,16]. ClO_2 is typically transformed into ClO_2^- through a single-electron oxidation process [17]. Recent studies used external energy to activate ClO_2 to produce reactive species, resulting in improved micropollutant abatement. For example, the excellent performance of the co-exposure of ClO_2 and ultraviolet radiation (UV) was reported in micropollutant abatement due to the high yield of reactive species [18,19].

ClO_2-based oxidation includes direct and activated ClO_2 oxidations. Though studies on ClO_2-based oxidation, especially on the direct ClO_2 oxidation, have been increasing over the past decade, there is still a limited understanding of these processes on micropollutant abatement, such as their kinetics, reactive sites, activation methods, and degradation pathways. The existing review about ClO_2 primarily focused on the reaction with (in)organic compounds in water treatment [17], pathogenic microbe inactivation in water treatment [20], antimicrobial food packaging [21], disposable ClO_2 wipes [22], and postharvest handling and food storage [23]. To the best of our knowledge, there is no comprehensive review on ClO_2-based oxidation in micropollutant abatement. Therefore, providing a comprehensive review of this technology is crucial for future research and application. In this review, we emphatically discussed (1) ClO_2 properties; (2) reaction kinetics, reactive sites, and degradation pathways in the directed ClO_2 oxidation; and (3) reaction kinetics and degradation pathways in the UV-activated ClO_2 oxidation.

2. ClO_2 Physicochemical Properties

ClO_2 is a green-yellowish gas and has a pungent odor similar to Cl_2. It is one of the few compounds in nature that exist almost entirely as monomeric free radicals due to a single unpaired electron [24]. The molecular weight and the standard oxidation state of Cl atoms in ClO_2 are 67.46 and +4, respectively. ClO_2 has a boiling point of 11 °C, a melting point of −59 °C, a density of 1.64 g mL^{-1} (liquid) at 0 °C [25], a water solubility of 3.0 g L^{-1} at 25 °C [17], and pKa value of 3.0. ClO_2 is strongly soluble in water and does not hydrolyze to any appreciable extent but remains in solution as a dissolved gas [26]. ClO_2 in aqueous solutions is quite stable when protected from light and kept cool, well-sealed, and slightly acidified (pH = 6). The ultraviolet absorption spectrum of ClO_2 solutions has broadband with a peak at 359 nm and a molar extinction coefficient of ~1250 M^{-1} cm^{-1} [27].

ClO_2 has a relatively short half-life and is highly volatile and explosive under concentrations of >10% in the air [28]. ClO_2 solution under concentrations of <~10 g L^{-1} will not produce sufficiently high vapor pressure for an explosive hazard. In water treatment practice, the concentrations of concentrated ClO_2 solution rarely exceed 4 g L^{-1}. Furthermore, ClO_2 cannot be compressed, stored, or transported under pressure and must be generated on-site [29]. Compared with the electrolysis method, the chemical method is more mature for ClO_2 production, which refers to the reactions of sodium chlorite ($NaClO_2$) or sodium chlorate ($NaClO_3$) with Cl_2, hydrochloric acid (HCl), or peroxydisulfate ($H_2S_2O_8$)

(Equations (1)–(3)). The reaction of $NaClO_2$ with an acid, such as HCl, has become an increasingly common method for ClO_2 production due to the operational difficulty and safety concerns of handling Cl_2 gas. Noted, to produce the same mass weight of ClO_2, hydrochloric-based ClO_2 production (Equation (2)) uses 1.25 times more $NaClO_2$ than chlorine-based (Equation (1)) or peroxydisulfate-based (Equation (3)) ClO_2 production.

$$2NaClO_2 + Cl_2 \rightarrow 2ClO_2 + 2NaCl \quad (1)$$

$$5NaClO_2 + 4HCl \rightarrow 4ClO_2 + 5NaCl + 2H_2O \quad (2)$$

$$2NaClO_2 + 4Na_2S_2O_8 \rightarrow 2ClO_2 + 2Na_2SO_4 \quad (3)$$

In the water, ClO_2 reacts first with other compounds to form ClO_2^- through a one-electron transfer reaction (Equation (4)), with the redox potential of 0.936 V [30]. The second reaction of the formed ClO_2^- transforming to Cl^- by gaining four electrons does not occur readily, due to the low reactivity of ClO_2^- (Equation (5)). In practice, fast oxidation predominates, and therefore, ClO_2^- will be the significant byproduct during ClO_2 disinfection/oxidation [31]. ClO^{3-} will be another byproduct because of its presence in proprietary solutions of ClO_2. ClO_2 accepts five electrons when thoroughly reduced to Cl^-, while Cl_2 accepts two electrons from the oxidation compounds (Equations (6) and (7)). Therefore, the oxidative capacity of ClO_2 is also approximately 2.5 times of Cl_2 on a weight basis.

$$ClO_2 + e^- \rightarrow ClO_2^- \quad (4)$$

$$ClO_2^- + 2H_2O + 4e^- \rightarrow Cl^- + 4OH \quad (5)$$

$$ClO_2 + 2H_2O + 5e^- \rightarrow Cl^- + 4OH^- \quad (6)$$

$$Cl_2 + 2e^- \rightarrow 2Cl^- \quad (7)$$

3. Direct ClO_2 Oxidation

3.1. Reaction Kinetics

The reaction kinetics between ClO_2 and micropollutants can be well described by second-order kinetic models (Equations (8) and (9)), referring to a first-order model in ClO_2 concentration and a first-order model in micropollutant concentration [32,33].

$$ClO_2 + MP \rightarrow \text{product} \quad (8)$$

$$\frac{d[MP]tot}{dt} = -k_{app}[MP]_{tot}[ClO_2] \quad (9)$$

where MP is an organic micropollutant; k_{app} is the apparent second-order rate constant for the overall reaction; $[ClO_2]$ and $[MP]_{tot}$ is the ClO_2 and MP concentration, respectively.

The reaction kinetics of antibiotics with ClO_2 depends on their molecular structures and pH. The k_{app} of antibiotics ranged from 1.2 to 1.3 $\times$ 10^6 M^{-1} s^{-1} at neutral pH, with a general order of tetracyclines (10^5–10^6) > triclosan (10^4–10^5) > sulfonamides (10^3–10^4) > macrolides (10^1–10^2) > fluoroquinolones (1–10^1) (Table 1). There is the aniline moiety in tetracyclines and sulfonamides and phenol moiety in triclosan, but the alkyl amine moiety in macrolides and fluoroquinolones. The results suggested that antibiotics with the aniline and phenol groups may be more vulnerable to ClO_2 attack than those with the alkyl amine. Furthermore, enrofloxacin and ofloxacin with tertiary amines on piperazine moieties reacted faster with ClO_2 than other fluoroquinolones with secondary amines on piperazine moieties [34]. However, the reactivity of the dimethylamino group in tetracycline to ClO_2 is higher than that of trimethylamine but lower than that of N,N-dimethylaniline [35]. The k_{app} of antibiotics was related to pH as well. A kinetic study demonstrated that the k_{app} of ciprofloxacin (belonging to fluoroquinolones) increased by more than three orders of magnitude from pH 4.48 to 9.55 [34]. Similarly, the k_{app} increased by more than 4 to 6 and 1.6 to 2.2 orders of magnitude from pH 2.5 to 10.5 and from

4.0 to 9.5 for the ClO_2 oxidation of tetracyclines and sulfonamides, respectively [35,36]. The large variation with pH could be attributed to the varying reactivity of antibiotic acid-base species toward ClO_2. An increase in pH led to a larger fraction of the deprotonated species (A^-), thus facilitating the reaction of antibiotics with ClO_2. Similar trends were also observed in fluoroquinolones [34] and tetracyclines [35], indicating that the deprotonation of these antibiotics as pH increases considerably favors their oxidation by ClO_2.

Table 1. Second-order rate constants (k_{app}) in the reaction of ClO_2 with micropollutants.

Compounds	k_{app} (M^{-1} s^{-1})	pH	T (°C)	References
fluoroquinolones				
Ciprofloxacin	1.2	7.0	-	[37]
Ciprofloxacin	7.9	7.0	22	[34]
Norfloxacin	1.3×10^1	7.0	22	[34]
Lomefloxacin	6.8	7.0	22	[34]
Ofloxacin	7.8×10^1	7.0	22	[34]
Pipemidic acid	1.5	7.0	22	[34]
Enrofloxacin	6.3×10^1	7.0	22	[34]
tetracyclines				
Tetracycline	1.3×10^6	7.0	22	[35]
Oxytetracycline	1.2×10^6	7.0	22	[35]
Chlorotetracycline	3.2×10^5	7.0	22	[35]
Iso-chlorotetracycline	2.2×10^5	7.0	22	[35]
sulfonamides				
Sulfamethoxazole	6.7×10^3	7.0	20	[15]
Sulfamethoxazole	7.9×10^3	7.0	-	[37]
Sulfamethoxazole	6.1×10^3	7.0	20	[36]
Sulfamethizole	3.9×10^3	7.0	20	[36]
Sulfadimethoxine	4.4×10^3	7.0	20	[36]
Sulfamethazine	4.1×10^3	7.0	20	[36]
Sulfamerazine	5.6×10^3	7.0	20	[36]
Sulfathiazole	2.6×10^4	7.0	20	[36]
macrolides				
Roxithromycin	2.2×10^2	7.0	20	[15]
Roxithromycin	8.8×10^1	7.0	-	[37]
triclosan				
Triclosan	7.1×10^4	~7.0	rt	[38]
Triclosan	6.3×10^5	7.0	-	[37]
antipyretic analgesics				
Antipyrine	4.8×10^{-1}	7.0	25	[39]
Propylphenazone	>100	7.4	20	[15]
Propylphenazone	1.1×10^1	7.0	25	[40]
Naproxen	6.1×10^2	7.0	-	[37]
Naproxen	10–100	7.4	20	[15]
Aminopyrine	1.3×10^5	7.0	25	[40]
Aminopyrine	>100	7.4	20	[15]
Diclofenac	1.1×10^4	7.0	20	[15]
Diclofenac	1.5×10^3	7.0	25	[33]
Diclofenac	1.1×10^4	7.0	-	[37]
Acetaminophen	2.1×10^5	7.0	-	[37]
Fenoprofen	<1	7.4	20	[15]
Ibuprofen	<0.1	8.0	-	[41]
β-blockers				
Atenolol	~1	8.0	-	[41]
Metoprolol	1.3	8.0	20	[42]
antiepileptics				
Carbamazepine	<0.1	8.0	-	[41]
psychostimulants				
Caffeine	<1	7.4	20	[15]
antineoplastics				
Ifosfamide	<1	7.4	20	[15]
Cyclophosphamide	<1	7.4	20	[15]
lipid regulators				
Gemfibrozil	5.9×10^1	7.0	-	[37]
Gemfibrozil	<10	7.4	20	[15]

-: not available; rt: room temperature.

In addition, the direct ClO_2 oxidation was applied for degrading other PPCPs such as antipyretic analgesics, β-blockers, antiepileptics, psychostimulants, antineoplastics, and lipid regulator. The k_{app} of antipyretic analgesics ranged from 4.8×10^{-1} to 2.1×10^{5} M^{-1} s^{-1} at neutral pH (Table 1). Among them, aminopyrine, diclofenac, and acetaminophen had the highest k_{app} due to the tertiary amine, aniline, and phenol moiety in their molecule, respectively. The second highest k_{app} was observed in propylphenazone with the heterocyclic amine moiety and naproxen with substituted benzene moiety. The remaining studied PPCPs were less reactivity towards ClO_2 (Table 1). These results implied that ClO_2 is a highly selective oxidant with respect to micropollutants with specific functional groups such as aniline, phenolic moieties, the second and tertiary amine, heterocyclic amine, aromatic nucleus.

3.2. Reactive Sites

Reactive sites of micropollutants during ClO_2 oxidation are determined by functional groups with the highest electron densities due to the one-electron transfer mechanism. As for PPCPs, the main reactive sites include piperazine group, sulfonyl amido group, amino group, aniline group, pyrazolone group and phenol group (Table 2). The N4 atom in the piperazine ring of fluoroquinolones was the specific site to be attacked by ClO_2 [34]. Similarly, He et al. [43,44] found the tertiary N4 amines and the secondary N4 amines with the highest $2FED_{HOMO}{}^{2}$ value in the piperazinyl group as the most vulnerable sites in the reactions between ClO_2 and the fluoroquinolones of fleroxacin and enoxacin. The sulfonyl amido-nitrogen of sulfonamides could be the main reaction site toward ClO_2 [36]. The reaction of three representative β-lactam antibiotics with ClO_2 starts with a single-electron transfer from the lone electron pair of the amino group to ClO_2 [45]. ClO_2 reacts with tetracyclines predominantly in the unprotonated dimethylamino group and deprotonated phenolic-diketone group [35]. Furthermore, the reactive site of triclosan was the phenol group during ClO_2 oxidation [37]. For antipyretic analgesics, the aniline group in diclofenac was the reactive site and acted as the electron-rich moieties during ClO_2 oxidation [37]. The N2 atom on the pyrazolone ring of antipyrine was vulnerable under the electrophilic reaction of ClO_2 due to its high electron cloud density [39]. However, the C=C double bond on the pyrazolone ring of isopropylphenazone and aminopyrine were the most reactive sites toward ClO_2 [40].

The main reactive sites of pesticides are the urea group and aromatic benzene ring of phenylurea and sulfonylurea herbicides, the sulfur center of ametryn and methiocarb, the amide group and the phosphinothioyl group of organophosphorus pesticides. For example, the primary attack on two phenylurea herbicides of diuron and chlortoluron by ClO_2 might be the electron-rich nitrogen atom on the ureic side-chain [46]. However, the aromatic benzene ring of isoproturon is vulnerable to the attack of ClO_2 [47]. Additionally, the degradation of two sulfonylurea herbicides of nicosulfuron and thifensulfuron methyl started with an attack on the urea groups by ClO_2 [48]. The main reactive site of ametryn herbicide and methiocarb pesticide during ClO_2 oxidation was the sulfur center in their molecules [47,49]. ClO_2 oxidation of two organophosphorus pesticides started with an attack on the amide group of azamethiphos and the phosphinothioyl group of dimethoate [16].

Table 2. Reactive sites and degradation pathways based on the intermediate products in the reaction of ClO_2 with micropollutants.

Micropollutants	Molecular Structure	Reactive Sites	Pathways	References
β-lactam antibiotics				
Amoxicillin	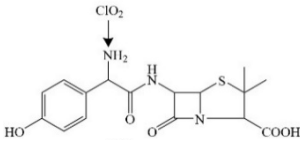	amino group	pathway: β-lactam ring breaking	[45]

Table 2. *Cont.*

Micropollutants	Molecular Structure	Reactive Sites	Pathways	References
Cefadroxil	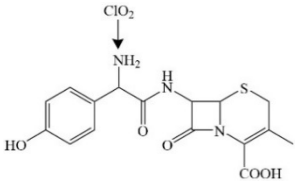			
fluoroquinolones				
Ciprofloxacin	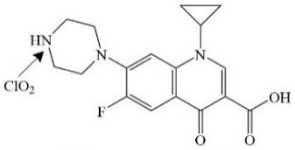	piperazine's N4 atom	pathway: dealkylation, hydroxylation and intramolecular ring closure at the piperazine moiety, and the quinolone ring mostly intact	[34]
Norfloxacin	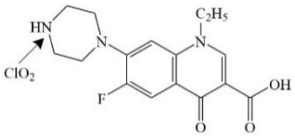			
Enoxacin	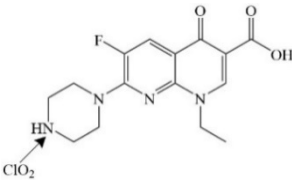		pathway: piperazine group cleavage, the decarboxylating quinolone ring, and hydroxylation	[44]
Fleroxacin	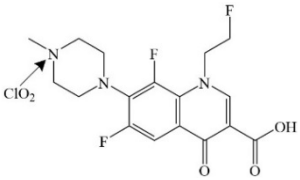		pathway: the cleavage of the piperazine ring and the decarboxylation and chlorination of the quinolone ring	[32]
sulfonamides				
Sulfamethoxazole	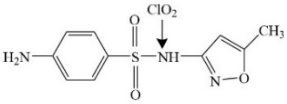	sulfonyl amido-nitrogen	pathway: breakage of S-N and C-S bonds and hydroxylation of aniline group	[36]
tetracyclines				
Tetracycline	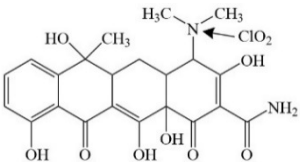	dimethylamino groups	pathway: (hydr)oxylation and breakage of tetracycline molecules	[35]
triclosan				
Triclosan	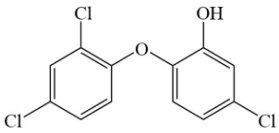	phenol group [a]	pathway: the closure of the phenolic ring, chlorination of the phenolic ring and cleavage of the ether bond	[38]
antipyretic analgesics				
Diclofenac	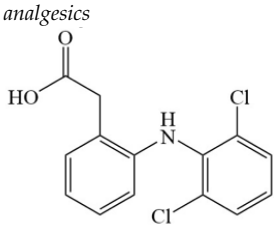	aniline group [a]	pathway: decarboxylation, hydroxylation and chlorination of the phenylacetic acid moiety, and further C-N bond cleavage	[50]

Table 2. *Cont.*

Micropollutants	Molecular Structure	Reactive Sites	Pathways	References
Antipyrine	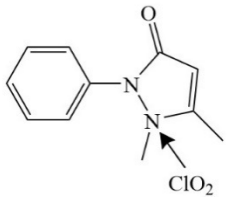	pyrazolone's N2 atom	pathway: chlorination substitution, ring-opening reaction and de-carbonyl reaction of the pyrazolone ring	[39]
Iso-propylphenazone	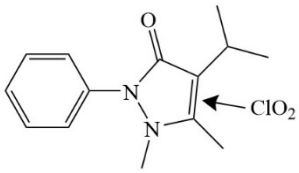	pyrazolone's C=C	pathway: C=C cleavage, ring opening reaction and de-carbonyl reaction of the pyrazolone ring	[40]
Aminopyrine	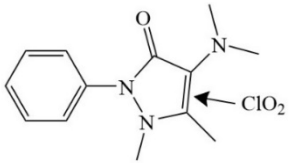			
antidepressant				
Venlafaxine	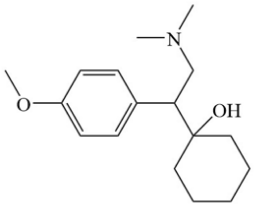	-	pathway: dehydration, demethylation and cleavage of the molecular structure	[51]
phenylurea herbicides				
Fenuron	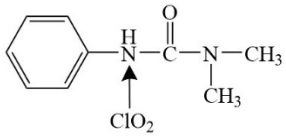	urea group	pathway: electrophilic substitution and cleavage of the urea group products: a chloro-quinone product and an urea derivative	[52]
Isoproturon	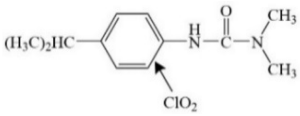	aromatic benzene ring	pathway: aromatic-ring hydroxylated substituted derivatives	[47]
Chlortoluron	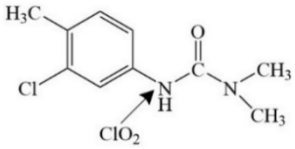	nitrogen atom on the ureic side-chain	pathway: radical intermediates formation, hydroxylation reactions and cleavage of the N–C bond on the ureic side-chain	[46]
Diuron	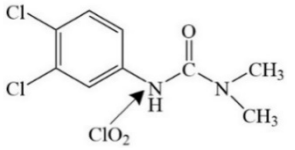		pathway: hydroxylation reactions and cleavage of the N–C bond on the ureic side-chain, dechloridation of the benzene ring	
sulfonylurea herbicides				
Nicosulfuron	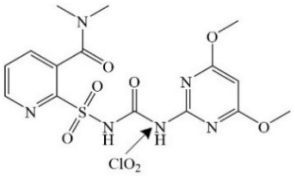	urea group	pathway: the urea group breaking	[48]

Table 2. *Cont.*

Micropollutants	Molecular Structure	Reactive Sites	Pathways	References
herbicide				
Ametryn	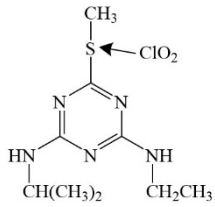	sulfur center	pathway: oxidation reactiveproduct: the sulphoxide derivative	[47]
carbamate pesticides				
Methiocarb	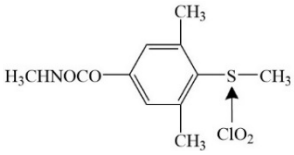	sulfur center	pathway: oxidation reaction products: methiocarb sulfoxidemethiocarb sulfone	[49]
organophosphorus pesticides				
Azamethiphos	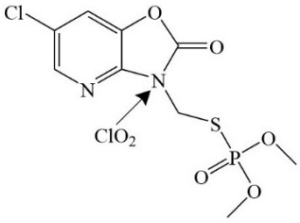	amide group	pathway: the breaking of amide group or S–C bond	[16]
Dimethoate	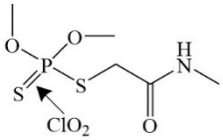	the phosphinothioyl group	pathway: the breaking of S–C bond, oxidation of the phosphinothioyl group	

[a] [37]; -: not available.

3.3. Degradation Pathways

One-electron transfer was the dominant degradation pathway in the direct ClO_2 oxidation of micropollutants, followed by indirect oxidation by oxygen species such as superoxide anion radical ($O_2^{\bullet -}$) or hydroxyl radical ($^{\bullet}OH$) (Figure 1). In detail, the one-electron transfer oxidation pathway refers to: (1) ClO_2 attacks the atom of the micropollutant with the highest electron density or the strongest electron-donating and takes away an electron from the atom to make micropollutant forming a radical intermediate ($MP^{\bullet}$), and is thus reduced to ClO_2^- (Equation (10); it is the rate-determining step) and (2) $MP^{\bullet}$ combines with another ClO_2 to form degradation products by undergoing molecular rearrangement and binding to itself or ClO_2 (Equation (11)). During the direct ClO_2 oxidization of $MP^{\bullet}$, the oxidant is initially reduced to ClO, then to HClO, and subsequently to Cl^-. Therefore, four tentative routes occur through the oxygen transfer process and potentially contribute to direct ClO_2 oxidization of micropollutants (Equations (12)–(15)), which were confirmed by the identification of decarbonyl-MP, hydroxyl-MP, chloro-MP, and even ring rupture of MP [38,53,54].

$$MP + ClO_2 \rightarrow MP^{\bullet} + ClO_2^- \quad (10)$$

$$MP^{\bullet} + ClO_2 \rightarrow \text{products} \quad (11)$$

$$MP^{\bullet} + ClO_2 \rightarrow MP - OH + ClO \quad (12)$$

$$MP^{\bullet} + ClO_2 \rightarrow \text{decarbonyl} - MP + ClO \quad (13)$$

$$MP^{\bullet} + H^+ + ClO \rightarrow MP^+ + HOCl \quad (14)$$

$$MP^{\bullet} + HOCl \rightarrow MP - Cl + H_2O \quad (15)$$

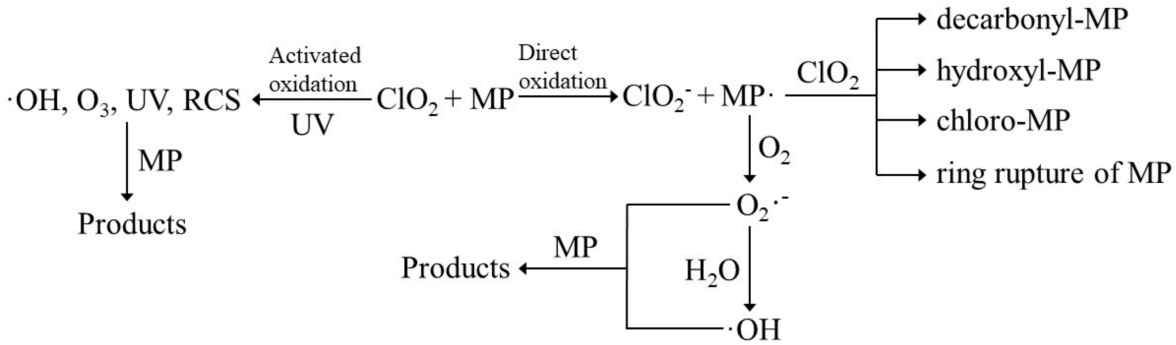

Figure 1. The degradation pathway of direct and activated ClO_2 oxidation for micropollutant abatement. RCS: $Cl^{\bullet}$, $ClO^{\bullet}$ and $Cl_2^{\bullet-}$; MP: micropollutant.

ClO_2 oxidation of PPCPs mainly led to the ring-opening reaction, dealkylation, decarboxylation, hydroxylation, and chlorination. The cleavage of the β-lactam ring in the molecules of penicillin, amoxicillin, and cefadroxil was observed in the ClO_2 oxidation of β-lactam antibiotics [45]. ClO_2 oxidation of fluoroquinolones, ciprofloxacin, and norfloxacin, led to dealkylation, hydroxylation, and intramolecular ring closure at the piperazine moiety but left the quinolone ring mostly intact [34]. Similarly, the primary and initial step in the ClO_2 oxidation of enoxacin and fleroxacin was the cleavage of the piperazine ring [32,44]. The decarboxylation and hydroxylation or chlorination of the quinolone ring occurred in enoxacin and fleroxacin, whereas the quinolone ring was unreactive of ciprofloxacin and norfloxacin. The cleavage of S−N and C−S bonds and the hydroxylation of aniline moiety were the major degradation pathways of sulfamethoxazole [36]. Furthermore, (hydr)oxylation and breakage of tetracycline were observed during the ClO_2 oxidation [35]. The pyrazolone ring-opening reaction caused by C=C double bond cleavage and further de-carbonyl reaction were the main degradation pathways of three antipyretic analgesics of antipyrine, isopropylphenazone, and aminopyrine [39,40]. ClO_2 oxidation of triclosan involved the cleavage of the ether link, chlorination of the phenolic ring, and ring closure [38]. The transformation pathways of venlafaxine included dehydration, demethylation, and cleavage of the molecule during ClO_2 oxidation [51].

ClO_2 reacts with commonly used phenylurea herbicides and sulfonylurea herbicides predominantly by the cleavage of the urea group and hydroxylated substitutes of the aromatic ring. ClO_2 oxidation of phenylurea herbicides of chlortoluron and diuron was subjected to steps including radical intermediates formation, hydroxylation reactions, and cleavage of the N−C bond on the ureic side-chain [46]. Isoproturon, a phenylurea-derivative, reacts with ClO_2 to form aromatic-ring hydroxylated substituted derivatives [47]. The urea group in sulfonylurea herbicide of nicosulfuron reacts firstly with ClO_2, resulting in breaking one bond and forming two degradation products of 2-(Nformylsulfamoyl)-N,N-dimethylnicotinamide and 4,6-dimethoxypyrimidin-2-amine [48].

Additionally, ClO_2 oxidation of other pesticides with the sulfur or phosphinothioyl center in their molecules led to sulfoxide and sulfone, ring rupture, hydroxylation, and decarbonyl products. Ametryn (R-S-CH3) reacted with ClO_2 forming the sulfoxide derivative (R-SO-CH3) [47]. Similarly, during the ClO_2 oxidation of the carbamate pesticide of methiocarb (MC), methiocarb sulfoxide and methiocarb sulfone were generated by losing $HClO_2$ and HOCl from the intermediate adduct of MC-ClO_2-OH, respectively, which was first formed around the sulfur center of methiocarb [49]. Pergal, et al. [16] studied the ClO_2 oxidation of two organophosphorus pesticides and found the successive attack on the amide group and the sulfide group in azamethiphos, leading to the break of the amide group and S–C bond, and the hydroxylation of the phosphinothioyl and then decarbonyl in dimethoate.

The indirect oxidation pathway of ClO_2 with micropollutants includes (1) the formation of $O_2^{\bullet-}$ by concurrently transferring an electron from $MP^{\bullet}$ to dissolved oxygen in solution (Equation (16)), (2) the reaction of $O_2^{\bullet-}$ with water with the formation of

$^{\bullet}OH$ (Equation (17)), and (3) the degradation of micropollutant by the formed $O_2^{\bullet-}/^{\bullet}OH$ (Equation (18)). For example, two major degradation pathways of diclofenac (DCF) were proposed as (1) direct ClO_2 oxidation through one-electron transfer and (2) indirect $O_2^{\bullet-}$ oxidation by concurrently transferring an electron from $DCF^{\bullet}$ to dissolved oxygen [33].

$$MP^{\bullet} + O_2 \rightarrow MP^{+} + O_2^{\bullet-} \quad (16)$$

$$O_2^{\bullet-} + H_2O \rightarrow {}^{\bullet}OH \quad (17)$$

$$MP + O_2^{\bullet-}/^{\bullet}OH \rightarrow \text{products} \quad (18)$$

4. UV-Activated ClO_2 Oxidation

4.1. Reaction Kinetics

The micropollutant abatements were generally enhanced by combining ClO_2 with shortwave ultraviolet light (UVC), which follows the pseudo-first-order reaction kinetics with the pseudo-first-order rates (k_{obs}) of 1.3×10^{-4}–9.8×10^{-3} s^{-1} at pH 7.0 (Table 3). For example, more than 99% of triclosan was degraded under co-exposure to UVC irradiation and ClO_2 [55]. Four micropollutants (i.e., trimethoprim, iopromide, caffeine, and ciprofloxacin) were degraded by 14.4–100.0% in UVC/ClO_2, with the corresponding k_{obs} following an order of ciprofloxacin (9.8×10^{-3} s^{-1}) > iopromide (1.2×10^{-3} s^{-1}) > trimethoprim (5.7×10^{-4} s^{-1}) > caffeine (1.3×10^{-4} s^{-1}) [18]. The degradation of these four micropollutants was accelerated in UVC/ClO_2, compared to direct ClO_2 oxidation or UVC photolysis. Ye et al. [56] reported that 95% flumequine was degraded ($k_{obs} = 2.7 \times 10^{-3}$ s^{-1}) in UVC/ClO_2 AOP, and its degradation rate gradually increased with ClO_2 dosage and UV intensity, but decreased as pH ascended. Though the combination of UVC and ClO_2 enhanced the micropollutant abatement via generating more reactive species (e.g., $^{\bullet}OH$ and chlorine radical ($Cl^{\bullet}$)), they are less effective than the well-documented UVC/H_2O_2, UVC/Cl_2, and UVC/NH_2Cl AOPs under the same initial oxidant dosages. For example, Tian et al. [57] compared the combination of UVC with different oxidants (i.e., Cl_2, NH_2Cl, ClO_2, and H_2O_2) in the degradation of iopamidol and reported the k_{obs} following the order of UVC/Cl_2 (1.9×10^{-2} s^{-1}) > UVC/H_2O_2 (1.3×10^{-2} s^{-1}) > UVC/NH_2Cl (1.0×10^{-2} s^{-1}) > UVC/ClO_2 (4.4×10^{-3} s^{-1}) under the same conditions.

Table 3. Summary of research studying the removal of micropollutants by the UV-activated ClO_2 oxidation.

Micropollutants	C_0	ClO_2	UV Light	Light Intensity	Reaction pH	k_{obs} (s^{-1})	Removal Rate (%)	References
Triclosan	0.3 mg L^{-1}	0.5 mg L^{-1}	UVC	6.5 μW cm^{-2}	~7.0	-	>99	[55]
Trimethoprim	1 μg L^{-1}	1.4 mg L^{-1}	UVC	207 mJ cm^{-2}	7.0	5.7×10^{-4}	14.4–100.0	[18]
Iopromide	1 μg L^{-1}	1.4 mg L^{-1}	UVC	207 mJ cm^{-2}	7.0	1.2×10^{-3}	14.4–100.0	[18]
Caffeine	1 μg L^{-1}	1.4 mg L^{-1}	UVC	207 mJ cm^{-2}	7.0	1.3×10^{-4}	14.4–100.0	[18]
Ciprofloxacin	1 μg L^{-1}	1.4 mg L^{-1}	UVC	207 mJ cm^{-2}	7.0	9.8×10^{-3}	14.4–100.0	[18]
Iopamidol	10 μM	200 μM	UVC	2.4 mW cm^{-2}	7.0	4.4×10^{-3}	74.9	[57]
Micropollutants [a]	1 μM	5 mg L^{-1}	UVA	0.3 mW cm^{-2}	7.0	3.8×10^{-4} to 12.9	7–100	[19]

-: not available; [a] 19 micropollutants: iopromide, trimethoprim, caffeine, 17α-ethynylestradiol, 17β-estradiol, estrone, diclofenac, sulfamethoxazole, gemfibrozil, naproxen, ofloxacin, roxithromycin, carbamazepine, metoprolol, atenolol, metronidazole, bezafibrate, clofibric acid, ibuprofenreported.

A novel UVC/ClO_2^- AOP was proposed to remove both ClO_2^- residue and micropollutants in water. UV photolysis after ClO_2 disinfection can effectively eliminate both ClO_2^- and carbamazepine by $^{\bullet}OH$ and reactive chlorine species (RCS) generated from UVC/ClO_2^- [58]. The $^{\bullet}OH$ generated from UVC/ ClO_2^- (Equations (19)–(21)) reacts with not only carbamazepine, but also ClO_2^- to generate ClO_2 (Equation (22)), which subsequently is activated by UV radiation to produce RCS (i.e., $Cl^{\bullet}$ and chlorine oxide radicals ($ClO^{\bullet}$)). As the products of UVC/ClO_2^-, Cl^- and ClO_3^- presented the decreasing and increasing yield, respectively, with the increasing ClO_2^- dosage [58]. Furthermore, Su et al., [59] developed a combined ClO_2^- photocatalysis technique for the degradation and detoxification of norfloxacin by dosing ClO_2^- in a visible light photocatalytic system.

The degradation rate of norfloxacin in the combined ClO_2^- photocatalysis system was faster than the single photocatalytic system or the single chlorite system under irradiation. The regenerated ClO_2^- can be retransformed into ClO_2 based on the ClO_2^-/ClO_2 dynamic interchange mechanism [59].

$$\text{photocatalysts} \rightarrow \text{photocatalysts}\ (h^+ + e^-) \tag{19}$$

$$O_2 + e^- \rightarrow O_2^{\bullet -} \tag{20}$$

$$O_2^{\bullet -} + H_2O \rightarrow {}^{\bullet}OH \tag{21}$$

$${}^{\bullet}OH + ClO_2^- \rightarrow ClO_2 + OH^- \ k = 6.3 \times 10^9\ M^{-1}\ s^{-1} \tag{22}$$

However, UVC/ClO_2 AOP suffer from several drawbacks: (1) low absorption of ClO_2 in the UVC range with the molar absorption coefficients of 60.7 M^{-1} cm^{-1} [19]; (2) high energy demand from UVC irradiation and low energy efficiency of low-pressure mercury ultraviolet (LPUV) lamps [19]; and (3) more emitted photons of UVC irradiation absorbed by background matrix components [27]. To address these issues, an emerging AOP combining longwave ultraviolet light (UVA) with ClO_2 (UVA/ClO_2) was proposed as an alternative to UVC/ClO_2 AOP because of the high molar absorptivity for ClO_2 at UVA wavelengths (ε359 nm = 1250 M^{-1} cm^{-1}), reduced photon absorption by background matrix components at 365 nm, and high energy efficiency of UVA-LEDs. Recently, a novel UVA/ClO^2 AOP was proposed as an alternative to UVC/H_2O_2 AOP [27]. Furthermore, the novel UVA/ClO_2 AOP was conducted for the degradation of 19 micropollutants with the degradation percentages of 7 to 100% and the corresponding k_{obs} of 3.8×10^{-4}–12.9 s^{-1} (Table 3) [19]. They also suggested that compared to UVC/Cl_2, UVA/ClO_2 AOP produced similar or higher levels of reactive species at similar oxidant dosages, required lower energy input, and formed lower Cl-DBPs.

4.2. Degradation Pathways

The associated radical chemistry of UV photolysis of ClO_2 is rather complicated, as demonstrated in Equations (23)–(32). Studies have reported that ClO_2 has strong absorption bands in the near-ultraviolet region, and photoexcitation of ClO_2 can lead to the breaking of the O−ClO bond by two active product channels. $ClO^{\bullet}$ and oxygen atoms ($O(^3P)$) [18] or excited state oxygen ($^1O_2$) [56] were proposed as the primary photo-fragments formed through the O−ClO bond breakage (Equation (23)). As for another channel, $Cl^{\bullet}$ and dissolved oxygen (O_2) were also observed from ClO_2 photolysis (Equation (24)) [27]. The generated product radicals $ClO^{\bullet}$, $O(^3P)/^1O_2$, and $Cl^{\bullet}$ from ClO_2 photolysis can undergo distinct chain reactions to generate secondary reactive species. $ClO^{\bullet}$ reacts rapidly with H_2O/HO^- to yield free chlorine ($HOCl/OCl^-$) (Equations (25) and (26)). $O(^3P)$ reacts rapidly with O_2 to produce ozone (O_3) (Equation (27)). The reactions of $Cl^{\bullet}$ with Cl^-, H_2O/HO^-, or $HOCl/OCl^-$ can form dichlorine radical anions ($Cl_2^{\bullet -}$) (Equation (28)), $HO^{\bullet}$ (Equations (29) and (30)), or $ClO^{\bullet}$ (Equations (31) and (32)) [18].

$$ClO_2 + hv \rightarrow ClO^{\bullet} + O(^3P)\ /\ 2ClO_2 + hv \rightarrow 2ClO^{\bullet} + {}^1O_2 \tag{23}$$

$$ClO_2 + hv \rightarrow ClOO \rightarrow Cl^{\bullet} + O_2 \tag{24}$$

$$2ClO^{\bullet} + H_2O \rightarrow HOCl + HClO_2\ k = 2.5 \times 10^9\ M^{-1}\ s^{-1} \tag{25}$$

$$2ClO^{\bullet} + HO^- \rightarrow OCl^- + HClO_2\ k = 2.5 \times 10^9\ M^{-1}\ s^{-1} \tag{26}$$

$$O(^3P) + O_2 \rightarrow O_3\ k = 4 \times 10^9\ M^{-1}\ s^{-1} \tag{27}$$

$$Cl^{\bullet} + Cl^- \rightarrow Cl_2^{\bullet -}\ k = 8.5 \times 10^9\ M^{-1}\ s^{-1} \tag{28}$$

$$Cl^{\bullet} + HO^- \rightarrow ClOH^{\bullet -}\ k = 1.8 \times 10^{10}\ M^{-1}\ s^{-1} \tag{29}$$

$$ClOH^{\bullet -} \rightarrow HO^{\bullet} + Cl^-\ k = 6.1 \times 10^9\ M^{-1}\ s^{-1} \tag{30}$$

$$Cl^{\bullet} + HOCl \rightarrow ClO^{\bullet} + H^{+} + Cl^{-} \; k = 3.0 \times 10^{9} \; M^{-1} \; s^{-1} \quad (31)$$

$$Cl^{\bullet} + OCl^{-} \rightarrow ClO^{\bullet} + Cl^{-} \; k = 8.3 \times 10^{9} \; M^{-1} \; s^{-1} \quad (32)$$

The degradation pathways of micropollutants in UV-activated ClO_2 oxidation include direct ClO_2 oxidation as discussed in Section 3.3, direct UV photolysis, ozonation, $^{\bullet}OH$-involved reactions, and RCS-involved reactions (i.e., $Cl^{\bullet}$, $ClO^{\bullet}$ and $Cl_2^{\bullet-}$) (Figure 1). Kong et al. [18] investigated the degradation pathways of four micropollutants of trimethoprim, iopromide, caffeine, and ciprofloxacin, with diverse chemical characteristics (i.e., caffeine bears electron-deficient moieties; trimethoprim and ciprofloxacin bear electron-rich moieties; iopromide bears photolabile moieties), during UVC/ClO_2. The degradation of caffeine was mainly caused by $Cl^{\bullet}$ (66.5%) and $^{\bullet}OH$ (33.5%), whereas the degradation of trimethoprim, iopromide, and ciprofloxacin were mainly contributed by ClO_2 oxidation (72.2%), UVC photolysis (87.1%), in situ formed free chlorine (84.3%), respectively (Table 4). The degradation of flumequine in UVC/ClO_2 was contributed by 11.37% UV photolysis, 14.72% $^1O_2$, 19.79% $^{\bullet}OH$, and 54.12% RCS (i.e., $Cl^{\bullet}$, $ClO^{\bullet}$ and $Cl_2^{\bullet-}$) (Table 4) [56]. The reaction pathways for the major species in UVA/ClO_2 AOP was recently well-summarized by Chuang et al. [27], which generates secondary reactive species such as $^{\bullet}OH$, $Cl_2^{\bullet-}$, and O_3 with relatively high and stable concentrations. Additionally, the contribution of reactive species on the removal of 19 micropollutants followed an order of O_3 > $ClO^{\bullet}$ > $HO^{\bullet}$ > $Cl^{\bullet}$ and their concentrations were $\sim 10^{-7}$, $\sim 10^{-13}$, $\sim 10^{-14}$, and $\sim 10^{-15}$ M, respectively, in UVA/ClO_2 at a ClO_2 dosage of 5 mg L^{-1} and a UV fluence of 47.5 mJ cm^{-2} (Table 4) [19].

Table 4. The contribution of reactive species for micropollutant abatement in UV/ClO_2 process.

Compounds	Contribution of Reactive Species	References
UVC-LPUV		
Trimethoprim	ClO_2 oxidation (72.2%) $^{\bullet}OH$ (11.5%) $Cl^{\bullet}$ (8.9%) Other reactive species [a] (7.5%)	[18]
Iopromide	UVC photolysis (87.1%) $^{\bullet}OH$ (2.0%) $Cl^{\bullet}$ (5.4%) Other reactive species [a] (5.5%)	
Caffeine	$Cl^{\bullet}$ (66.5%) $^{\bullet}OH$ (33.5%)	
Ciprofloxacin	ClO_2 oxidation (6.9%) UVC photolysis (8.0%) $Cl^{\bullet}$ (0.3%) $^{\bullet}OH$ (0.5%) in-situ formed free chlorine (84.3%)	
UVC-LPUV		
Flumequine	UVC photolysis (11.37%) $^1O_2$ (14.72%) $^{\bullet}OH$ (19.79%) RCS [b] (54.12%)	[56]
UVA-LEDs		
Micropollutants [c]	$ClO^{\bullet}$ ($\sim 10^{-13}$ M) $Cl^{\bullet}$ ($\sim 10^{-15}$ M) $^{\bullet}OH$ ($\sim 10^{-14}$ M) Ozone ($\sim 10^{-7}$ M)	[19]

[a] other reactive species: $O(^3P)$, $ClO^{\bullet}$, O_3, $Cl_2^{\bullet-}$, and/or in-situ formed chlorine. [b] RCS: $Cl^{\bullet}$, $ClO^{\bullet}$ and $Cl_2^{\bullet-}$. [c] 19 micropollutants: iopromide, trimethoprim, caffeine, 17α-ethynylestradiol, 17β-estradiol, estrone, diclofenac, sulfamethoxazole, gemfibrozil, naproxen, ofloxacin, roxithromycin, carbamazepine, metoprolol, atenolol, metronidazole, bezafibrate, clofibric acid, ibuprofenreported.

5. Research Gap and Future Research

Compared to UVC/ClO_2 AOP, UVA/ClO_2 AOP is practically promising for micropollutant abatement due to high absorption coefficients of ClO_2 in the UVA range, reduced photon absorption by the background matrix components, and high energy efficiency of UVA-LEDs. However, up until now, reports regarding degradation efficiency, degradation products, degradation pathways, reactive species, influencing factors (e.g., ClO_2 concentration, UV intensity, pH, and water matrices), and DBP formation are still limited during micropollutant abatement by UVA/ClO_2. Although the formation of halogenated DBPs during ClO_2-based oxidation is limited, inorganic products (i.e., ClO_2^-, ClO_3^-, and Cl^-) might be a new concern when this technology is used in micropollutant abatement in water. Studies reported that the inorganic products were comprised of 50 to 70% of ClO_2^- and 30 to 50% of ClO_3^- and Cl^- in direct ClO_2 oxidation. However, research regarding the yield of ClO_2^-, ClO_3^-, and Cl^- in activated ClO_2 oxidation and influencing factors (e.g., ClO_2 dosage, pH, activation methods, and water matrices) on inorganic products in both direct ClO_2 oxidation and activated ClO_2 oxidation remain unclear. Recently, studies have reported that carbamazepine and norfloxacin were degraded by $^{\bullet}OH$ and RCS generated from a novel UVC/ClO_2^- system, providing a possibility of "killing two birds with one stone": eliminating both ClO_2^- residue and micropollutants. However, up until now, degradation efficiency, degradation products, degradation pathways, influencing factors (e.g., ClO_2^- concentration, UV intensity, pH, and water matrixes), reactive species, formation of organic or inorganic DBPs, and ClO_2^-/ClO_2 dynamic interchange are still limited.

Author Contributions: Writing—original draft preparation, X.M.; writing—review and editing, X.M., H.C., X.H. and R.C.; validation, X.M. and R.C. All authors have read and agreed to the published version of the manuscript.

Funding: This project was supported by the National Natural Science Foundation of China (52100200), the United States Department of Agriculture-National Institute of Food and Agriculture (USDA-NIFA, 2020-67019-31022, 2021-67019-33682, and 2022-67019-37177), Gansu Provincial Youth Science and Technology Planning Project (20JR10RA109) and the Scientific Research Ability Promotion plan of Young Teachers from Northwest Normal University (NWNU-LKQN2019-31).

Institutional Review Board Statement: Not applicable.

Informed Consent Statement: Not applicable.

Data Availability Statement: Not applicable.

Conflicts of Interest: The authors declare no conflict of interest.

References

1. Lado Ribeiro, A.R.; Moreira, N.F.F.; Li Puma, G.; Silva, A.M.T. Impact of water matrix on the removal of micropollutants by advanced oxidation technologies. *Chem. Eng. J.* **2019**, *363*, 155–173. [CrossRef]
2. Gorito, A.M.; Pesqueira, J.F.J.R.; Moreira, N.F.F.; Ribeiro, A.R.; Pereira, M.F.R.; Nunes, O.C.; Almeida, C.M.R.; Silva, A.M.T. Ozone-based water treatment (O_3, O_3/UV, O_3/H_2O_2) for removal of organic micropollutants, bacteria inactivation and regrowth prevention. *J. Environ. Chem. Eng.* **2021**, *9*, 105315. [CrossRef]
3. Borrull, J.; Colom, A.; Fabregas, J.; Borrull, F.; Pocurull, E. Presence, behaviour and removal of selected organic micropollutants through drinking water treatment. *Chemosphere* **2021**, *276*, 130023. [CrossRef] [PubMed]
4. Li, R.; Kadrispahic, H.; Koustrup Jørgensen, M.; Brøndum Berg, S.; Thornberg, D.; Mielczarek, A.T.; Bester, K. Removal of micropollutants in a ceramic membrane bioreactor for the post-treatment of municipal wastewater. *Chem. Eng. J.* **2022**, *427*, 131458. [CrossRef]
5. Xu, L.; Wu, C.; Chai, C.; Cao, S.; Bai, X.; Ma, K.; Jin, X.; Shi, X.; Jin, P. Adsorption of micropollutants from wastewater using iron and nitrogen co-doped biochar: Performance, kinetics and mechanism studies. *J. Hazard. Mater.* **2022**, *424*, 127606. [CrossRef]
6. Kiejza, D.; Kotowska, U.; Polińska, W.; Karpińska, J. Peracids—New oxidants in advanced oxidation processes: The use of peracetic acid, peroxymonosulfate, and persulfate salts in the removal of organic micropollutants of emerging concern—A review. *Sci. Total Environ.* **2021**, *790*, 148195. [CrossRef]
7. Mukherjee, A.; Mullick, A.; Moulik, S.; Roy, A. Oxidative degradation of emerging micropollutants induced by rotational hydrodynamic cavitating device: A case study with ciprofloxacin. *J. Environ. Chem. Eng.* **2021**, *9*, 105652. [CrossRef]

8. Tagliavini, M.; Schäfer, A.I. Removal of steroid micropollutants by polymer-based spherical activated carbon (PBSAC) assisted membrane filtration. *J. Hazard. Mater.* **2018**, *353*, 514–521. [CrossRef]
9. Ao, X.W.; Eloranta, J.; Huang, C.H.; Santoro, D.; Sun, W.J.; Lu, Z.D.; Li, C. Peracetic acid-based advanced oxidation processes for decontamination and disinfection of water: A review. *Water Res.* **2021**, *188*, 116479. [CrossRef]
10. Malvestiti, J.A.; Cruz-Alcalde, A.; López-Vinent, N.; Dantas, R.F.; Sans, C. Catalytic ozonation by metal ions for municipal wastewater disinfection and simulataneous micropollutants removal. *Appl. Catal. B-Environ.* **2019**, *259*, 118104. [CrossRef]
11. Mei, L.; Shilong, T.; Jin, S.; Xizhuo, W.; Jianxin, C.; Shouqiang, L.; Xia, G.; Jiachun, T. Effects of chlorine dioxide on morphology and ultrastructure of Fusarium sulphureum and its virulence to potato tubers. *Int. J. Agric. Biol. Eng.* **2017**, *10*, 242–250. [CrossRef]
12. Han, J.; Zhang, X.; Li, W.; Jiang, J. Low chlorine impurity might be beneficial in chlorine dioxide disinfection. *Water Res.* **2021**, *188*, 116520. [CrossRef] [PubMed]
13. Maeda, Y. Roles of Sulfites in Reverse Osmosis (RO) Plants and Adverse Effects in RO Operation. *Membranes* **2022**, *12*, 170. [CrossRef] [PubMed]
14. Rougé, V.; Allard, S.; Croué, J.P.; von Gunten, U. In-situ formation of free chlorine during ClO_2 treatment: Implications on the formation of disinfection by-products. *Environ. Sci. Technol.* **2018**, *52*, 13421–13429. [CrossRef]
15. Huber, M.M.; Korhonen, S.; Ternes, T.A.; von Gunten, U. Oxidation of pharmaceuticals during water treatment with chlorine dioxide. *Water Res.* **2005**, *39*, 3607–3617. [CrossRef]
16. Pergal, M.V.; Kodranov, I.D.; Dojcinovic, B.; Avdin, V.V.; Stankovic, D.M.; Petkovic, B.B.; Manojlovic, D.D. Evaluation of azamethiphos and dimethoate degradation using chlorine dioxide during water treatment. *Environ. Sci. Pollut. Res. Int.* **2020**, *27*, 27147–27160. [CrossRef]
17. Gan, W.H.; Ge, Y.X.; Zhong, Y.; Yang, X. The reactions of chlorine dioxide with inorganic and organic compounds in water treatment: Kinetics and mechanisms. *Environ. Sci. Water Res.* **2020**, *6*, 2287–2312. [CrossRef]
18. Kong, Q.; Fan, M.; Yin, R.; Zhang, X.; Lei, Y.; Shang, C.; Yang, X. Micropollutant abatement and byproduct formation during the co-exposure of chlorine dioxide (ClO_2) and UVC radiation. *J. Hazard. Mater.* **2021**, *419*, 126424. [CrossRef]
19. Peng, J.; Yin, R.; Yang, X.; Shang, C. A Novel UVA/ClO_2 Advanced Oxidation Process for the Degradation of Micropollutants in Water. *Environ. Sci. Technol.* **2022**, *56*, 1257–1266. [CrossRef]
20. Ge, Y.; Zhang, X.; Shu, L.; Yang, X. Kinetics and Mechanisms of Virus Inactivation by Chlorine Dioxide in Water Treatment: A Review. *Bull. Environ. Contam. Toxicol.* **2021**, *106*, 560–567. [CrossRef]
21. Singh, S.; Maji, P.K.; Lee, Y.S.; Gaikwad, K.K. Applications of gaseous chlorine dioxide for antimicrobial food packaging: A review. *Environ. Chem. Lett.* **2020**, *19*, 253–270. [CrossRef]
22. Tofanelli, M.; Capriotti, V.; Saraniti, C.; Marcuzzo, A.V.; Boscolo-Rizzo, P.; Tirelli, G. Disposable chlorine dioxide wipes for high-level disinfection in the ENT department: A systematic review. *Am. J. Otolaryngol.* **2020**, *41*, 102415. [CrossRef] [PubMed]
23. Sun, X.; Baldwin, E.; Bai, J. Applications of gaseous chlorine dioxide on postharvest handling and storage of fruits and vegetables—A review. *Food Control* **2019**, *95*, 18–26. [CrossRef]
24. McCarthy, W.P.; O'Callaghan, T.F.; Danahar, M.; Gleeson, D.; O'Connor, C.; Fenelon, M.A.; Tobin, J.T. Chlorate and Other Oxychlorine Contaminants Within the Dairy Supply Chain. *Compr. Rev. Food Sci. Food Saf.* **2018**, *17*, 1561–1575. [CrossRef]
25. Kessler, S.J. Shelf Life Extension of Fresh Strawberries Packaged in Clamshells with Chlorine Dioxide Generating Sachets. Ph.D. Thesis, Clemson University, Clemson, SC, USA, 2020.
26. Champ, T.B.; Jang, J.H.; Lee, J.L.; Wu, G.; Reynolds, M.A.; Abu-Omar, M.M. Lignin-Derived Non-Heme Iron and Manganese Complexes: Catalysts for the On-Demand Production of Chlorine Dioxide in Water under Mild Conditions. *Inorg. Chem.* **2021**, *60*, 2905–2913. [CrossRef]
27. Chuang, Y.H.; Wu, K.L.; Lin, W.C.; Shi, H.J. Photolysis of Chlorine Dioxide under UVA Irradiation: Radical Formation, Application in Treating Micropollutants, Formation of Disinfection Byproducts, and Toxicity under Scenarios Relevant to Potable Reuse and Drinking Water. *Environ. Sci. Technol.* **2022**, *56*, 2593–2604. [CrossRef]
28. Kim, H.; Lee, J.; Sadeghi, K.; Seo, J. Controlled self-release of ClO_2 as an encapsulated antimicrobial agent for smart packaging. *Innov. Food Sci. Emerg.* **2021**, *74*, 102802. [CrossRef]
29. Trinh, V.M.; Yuan, M.H.; Chen, Y.H.; Wu, C.Y.; Kang, S.C.; Chiang, P.C.; Hsiao, T.C.; Huang, H.P.; Zhao, Y.L.; Lin, J.F.; et al. Chlorine dioxide gas generation using rotating packed bed for air disinfection in a hospital. *J. Clean. Prod.* **2021**, *320*, 128885. [CrossRef]
30. Mao, Q.; Li, Q.; Li, H.; Yuan, S.; Zhang, J. Oxidative paraben removal with chlorine dioxide: Reaction kinetics and mechanism. *Sep. Purif. Technol.* **2020**, *237*, 116327. [CrossRef]
31. Hupperich, K.; Mutke, X.A.M.; Abdighahroudi, M.S.; Jütte, M.; Schmidt, T.C.; Lutze, H.V. Reaction of chlorine dioxide with organic matter—Formation of inorganic products. *Environ. Sci. Water Res.* **2020**, *6*, 2597–2606. [CrossRef]
32. He, G.; Zhang, T.; Li, Y.; Li, J.; Chen, F.; Hu, J.; Dong, F. Comparison of fleroxacin oxidation by chlorine and chlorine dioxide: Kinetics, mechanism and halogenated DBPs formation. *Chemosphere* **2022**, *286*, 131585. [CrossRef] [PubMed]
33. Wang, Y.; Liu, H.; Xie, Y.; Ni, T.; Liu, G. Oxidative removal of diclofenac by chlorine dioxide: Reaction kinetics and mechanism. *Chem. Eng. J.* **2015**, *279*, 409–415. [CrossRef]
34. Wang, P.; He, Y.L.; Huang, C.H. Oxidation of fluoroquinolone antibiotics and structurally related amines by chlorine dioxide: Reaction kinetics, product and pathway evaluation. *Water Res.* **2010**, *44*, 5989–5998. [CrossRef] [PubMed]

35. Wang, P.; He, Y.L.; Huang, C.H. Reactions of tetracycline antibiotics with chlorine dioxide and free chlorine. *Water Res.* **2011**, *45*, 1838–1846. [CrossRef]
36. Ben, W.W.; Shi, Y.W.; Li, W.W.; Zhang, Y.; Qiang, Z.M. Oxidation of sulfonamide antibiotics by chlorine dioxide in water: Kinetics and reaction pathways. *Chem. Eng. J.* **2017**, *327*, 743–750. [CrossRef]
37. Lee, Y.; von Gunten, U. Quantitative structure-activity relationships (QSARs) for the transformation of organic micropollutants during oxidative water treatment. *Water Res.* **2012**, *46*, 6177–6195. [CrossRef] [PubMed]
38. Li, Q.S.; Yu, J.W.; Chen, W.Z.; Ma, X.Y.; Li, G.X.; Chen, G.Y.; Deng, J. Degradation of triclosan by chlorine dioxide: Reaction mechanism,2,4-dichlorophenol accumulation and toxicity evaluation. *Chemosphere* **2018**, *207*, 449–456. [CrossRef]
39. Jia, X.H.; Feng, L.; Liu, Y.Z.; Zhang, L.Q. Oxidation of antipyrine by chlorine dioxide: Reaction kinetics and degradation pathway. *Chem. Eng. J.* **2017**, *309*, 646–654. [CrossRef]
40. Jia, X.H.; Feng, L.; Liu, Y.Z.; Zhang, L.Q. Degradation behaviors and genetic toxicity variations of pyrazolone pharmaceuticals during chlorine dioxide disinfection process. *Chem. Eng. J.* **2018**, *345*, 156–164. [CrossRef]
41. Lee, Y.; von Gunten, U. Oxidative transformation of micropollutants during municipal wastewater treatment: Comparison of kinetic aspects of selective (chlorine, chlorine dioxide, ferrate VI, and ozone) and non-selective oxidants (hydroxyl radical). *Water Res.* **2010**, *44*, 555–566. [CrossRef]
42. Terhalle, J.; Kaiser, P.; Jutte, M.; Buss, J.; Yasar, S.; Marks, R.; Uhlmann, H.; Schmidt, T.C.; Lutze, H.V. Chlorine dioxide—Pollutant transformation and formation of hypochlorous acid as a secondary oxidant. *Environ. Sci. Technol.* **2018**, *52*, 9964–9971. [CrossRef]
43. He, G.L.; Zhang, T.Q.; Zheng, F.F.; Li, C.; Zhang, Q.Z.; Dong, F.L.; Huang, Y. Reaction of fleroxacin with chlorine and chlorine dioxide in drinking water distribution systems: Kinetics, transformation mechanisms and toxicity evaluations. *Chem. Eng. J.* **2019**, *374*, 1191–1203. [CrossRef]
44. He, G.; Zhang, T.; Zhang, Q.; Dong, F.; Wang, Y. Characterization of enoxacin (ENO) during ClO_2 disinfection in water distribution system: Kinetics, byproducts, toxicity evaluation and halogenated disinfection byproducts (DBPs) formation potential. *Chemosphere* **2021**, *283*, 131251. [CrossRef] [PubMed]
45. Navalon, S.; Alvaro, M.; Garcia, H. Reaction of chlorine dioxide with emergent water pollutants: Product study of the reaction of three beta-lactam antibiotics with ClO_2. *Water Res.* **2008**, *42*, 1935–1942. [CrossRef] [PubMed]
46. Tian, F.X.; Xu, B.; Zhang, T.Y.; Gao, N.Y. Degradation of phenylurea herbicides by chlorine dioxide and formation of disinfection by-products during subsequent chlor(am)ination. *Chem. Eng. J.* **2014**, *258*, 210–217. [CrossRef]
47. Lopez, A.; Mascolo, G.; Tiravanti, G.; Passino, R. Degradation of herbicides (ametryn and isoproturon) during water disinfection by means of two oxidants (hypochlorite and chlorine dioxide). *Water Sci. Technol.* **1997**, *35*, 129–136. [CrossRef]
48. Pergal, M.V.; Kodranov, I.D.; Pergal, M.M.; Dojčinović, B.P.; Stanković, D.M.; Petković, B.B.; Manojlović, D.D. Assessment of Degradation of Sulfonylurea Herbicides in Water by Chlorine Dioxide. *Water Air Soil Poll.* **2018**, *229*, 287. [CrossRef]
49. Tian, F.; Qiang, Z.; Liu, C.; Zhang, T.; Dong, B. Kinetics and mechanism for methiocarb degradation by chlorine dioxide in aqueous solution. *Chemosphere* **2010**, *79*, 646–651. [CrossRef]
50. Wang, Y.; Liu, H.; Liu, G.; Xie, Y. Oxidation of diclofenac by aqueous chlorine dioxide: Identification of major disinfection byproducts and toxicity evaluation. *Sci. Total Environ.* **2014**, *473–474*, 437–445. [CrossRef]
51. Lv, J.; Ou, C.; Fu, M.; Xu, Z. Characteristics and transformation pathways of venlafaxine degradation during disinfection processes using free chlorine and chlorine dioxide. *Chemosphere* **2021**, *276*, 130147. [CrossRef]
52. Benitez, F.J.; Beltran-Heredia, J.; Gonzalez, T.; Lara, P. Oxidation of Fenuron by chlorine dioxide. *J. Environ. Sci. Health A* **1992**, *27*, 643–662. [CrossRef]
53. Ali, O.A.; Tarek, S.J. Removal of polycyclic aromatic hydrocarbons from Ismailia Canal water by chlorine, chlorine dioxide and ozone. *Desalin. Water Treat.* **2009**, *1*, 289–298. [CrossRef]
54. Hey, G.; Grabic, R.; Ledin, A.; la Cour Jansen, J.; Andersen, H.R. Oxidation of pharmaceuticals by chlorine dioxide in biologically treated wastewater. *Chem. Eng. J.* **2012**, *185–186*, 236–242. [CrossRef]
55. Li, Q.S.; Cai, H.W.; Li, G.X.; Chen, G.Y.; Ma, X.Y.; He, W.L. Degradation behavior of triclosan by co-exposure to chlorine dioxide and UV irradiation: Influencing factors and toxicity changes. *Environ. Sci. Pollut. Res. Int.* **2018**, *25*, 9391–9401. [CrossRef]
56. Ye, W.K.; Tian, F.X.; Xu, B.; Zhao, D.S.; Ye, J.; Wang, B.; Lai, F.; Tan, Y.J.; Hu, X.J. Insights into the enhanced degradation of flumequine by UV/ClO_2 integrated process: Kinetics, mechanisms and DBPs-related toxicity in post-disinfection. *Sep. Purif. Technol.* **2022**, *280*, 119846. [CrossRef]
57. Tian, F.X.; Ye, W.K.; Xu, B.; Hu, X.J.; Ma, S.X.; Lai, F.; Gao, Y.Q.; Xing, H.B.; Xia, W.H.; Wang, B. Comparison of UV-induced AOPs (UV/Cl_2, UV/NH_2Cl, UV/ClO_2 and UV/H_2O_2) in the degradation of iopamidol: Kinetics, energy requirements and DBPs-related toxicity in sequential disinfection processes. *Chem. Eng. J.* **2020**, *398*, 125570. [CrossRef]
58. Wang, J.; Wu, Y.; Bu, L.; Zhu, S.; Zhang, W.; Zhou, S.; Gao, N. Simultaneous removal of chlorite and contaminants of emerging concern under UV photolysis: Hydroxyl radicals vs. chlorate formation. *Water Res.* **2021**, *190*, 116708. [CrossRef]
59. Su, R.; Huang, L.; Li, N.; Li, L.; Jin, B.; Zhou, W.; Gao, B.; Yue, Q.; Li, Q. Chlorine dioxide radicals triggered by chlorite under visible-light irradiation for enhanced degradation and detoxification of norfloxacin antibiotic: Radical mechanism and toxicity evaluation. *Chem. Eng. J.* **2021**, *414*, 128768. [CrossRef]